Polymer nanosieve membranes for CO2-capture applications

Du, Naiying; Park, Ho Bum; Robertson, Gilles P.; Dal-Cin, Mauro M.; Visser, Tymen; Scoles, Ludmila; Guiver, Michael D.

Publisher's version / Version de l'éditeur:
https://doi.org/10.1038/NMAT2989
Nature Materials, 10, pp. 372-375, 2011-04-03

LETTERS
PUBLISHED ONLINE: 3 APRIL 2011 | DOI: 10.1038/NMAT2989
nature materials

Polymer nanosieve membranes for CO_2-capture applications

Naiying Du[1†], Ho Bum Park[2†], Gilles P. Robertson[1], Mauro M. Dal-Cin[1], Tymen Visser[3], Ludmila Scoles[1] and Michael D. Guiver[1,2*]

Microporous organic polymers (MOPs) are of potential technological significance for gas storage[1–3], gas separation[4] and low-dielectric applications[5]. Among many approaches for obtaining such materials, solution-processable MOPs derived from rigid and contorted macromolecular structures are promising because of their excellent mass transport and mass exchange capability. Here we show a class of amorphous MOP, prepared by [2 + 3] cycloaddition modification of a polymer containing an aromatic nitrile group with an azide compound, showing super-permeable characteristics and outstanding CO_2 separation performance, even under polymer plasticization conditions such as CO_2/light gas mixtures. This unprecedented result arises from the introduction of tetrazole groups into highly microporous polymeric frameworks, leading to more favourable CO_2 sorption with superior affinity in gas mixtures, and selective CO_2 transport by presorbed CO_2 molecules that limit access by other light gas molecules. This strategy provides a direction in the design of MOP membrane materials for economic CO_2 capture processes.

MOPs are of great interest because they combine the processability of polymers with porous materials having high surface areas (300–1,500 $m^2\ g^{-1}$) comparable to typical microporous solids such as zeolites and activated carbons[6–8]. MOPs can be classified either as amorphous polymers (for example, substituted polyacetylenes[9], thermally rearranged (TR) polymers[4,10], and polymers of intrinsic microporosity (PIMs; refs 3,11)) or as crystalline polymers[12,13] (for example, covalent organic frameworks). Depending on the cavity size and shape, surface area and regularity, MOPs can be tailored for versatile applications. For membrane-based gas separation, solution-processable, amorphous MOPs are required for practical membrane fabrication such as thin-film composites. Among MOPs, poly(1-trimethylsilyl-1-propyne) (PTMSP) is known as the highest gas-permeable polymer. However, PTMSP shows low gas selectivity (for example, $CO_2/N_2 = 5.4$ and $CO_2/CH_4 = 2.1$; ref. 9), and also suffers from fast physical ageing, leading to a catastrophic reduction in gas permeability, because the initially formed microporous structures are rapidly corrupted by equilibrium processes. Recently, PIMs have attracted keen interest because they exhibit relatively slow physical ageing, good solubility, high gas permeability, as well as high selectivity[11,14–17] compared to PTMSP, resulting in gas separation performance that defines the upper bound of common organic polymers[18]. In general, PIMs have a structural combination of rigid ladder-like backbones with sites of contortion, which prevent intra- and/or inter-chain packing and create large free-volume elements. Accordingly, it is desirable to expand the structural variety of PIMs to better understand the structure–property relationships, which will lead to improved and tailored MOPs for membrane-based gas separation.

Separation of gas pairs in polymeric membranes is defined by the selectivity, $\alpha_{A/B}$, which is the ratio of the permeability of the faster gas (P_A) to the slower gas (P_B): $\alpha_{A/B} = P_A/P_B$. Selectivity can be decoupled into solubility-selectivity and diffusivity-selectivity, $\alpha_{A/B} = S_A/S_B \times D_A/D_B$. An improvement in selectivity can be achieved by a combination of greater gas diffusivity selectivity or increasing the solubility of the faster gas in the polymer. Previous work has attempted to increase the selectivity mainly by improving diffusivity-selectivity through an increase in the chain rigidity or by tuning cavity size[4,10]. On the other hand, increasing the solubility-selectivity of the 'faster gas' has also attracted great interest[19,20]. As such, even modest increases in solubility-selectivity can lead to significant improvements in overall selectivity.

Recently, the interactions between CO_2 and N-containing organic heterocyclic molecules such as pyridine, imidazole and tetrazole have been studied[21], revealing that Lewis acid–Lewis base interactions are most important, as is hydrogen bonding with the negatively charged oxygen atoms of CO_2. Thus, the incorporation of such heterocyclics into MOPs will play a major role in interacting with CO_2 to increase its solubility more than other gases. Central to our approach for improving CO_2 separation in MOPs is to combine CO_2-philic functional groups into MOPs, via a post-polymerization method. Here we demonstrate MOPs functionalized with CO_2-philic pendant tetrazole groups (hereafter referred to as TZPIMs). TZPIMs are of interest for their potential to yield both high CO_2 permeability and high CO_2/light gas selectivity because of the presence of strongly CO_2-sorbing tetrazole heterocyclic rings bound to a highly porous polymer matrix. Strongly bound CO_2 molecules in TZPIMs lead to a narrower cavity size that impedes the less-sorbed light gases, thereby hindering their transport in a mixed gas environment.

In this work, PIM-1 was selected as a MOP platform for post-polymerization modification owing to its simple structure, ease of preparation, high molecular weight and good mechanical strength. PIM-1 contains two nitrile groups per repeat unit, which is the reaction site for functionalization (Fig. 1a). The [2 + 3] cycloaddition post-polymerization reaction between nitriles and azides, so called 'click chemistry', leads to tetrazoles ($pK_a = 4.89$) having both basic character and an acidic hydrogen. Nitrile cycloadditions with azides are an uncommon variation of the better-known Huisgen 1,3-dipolar cycloaddition between terminal acetylenes and azides[22,23]. Recently, 'click chemistry' has been explored as a simple way for the functionalization of macromolecules[24–26]. Similar to the $ZnCl_2$-catalyzed 'click reaction' between azide and

[1]Institute for Chemical Process and Environmental Technology, National Research Council of Canada, Ottawa, Ontario K1A 0R6, Canada, [2]WCU Department of Energy Engineering, Hanyang University, Seoul 133-791, Republic of Korea, [3]Vaperma, 2111, 4e rue, St-Romuald, Québec, G6W 5M6, Canada. †These authors contributed equally to this work. *e-mail: michael.guiver@nrc-cnrc.gc.ca.

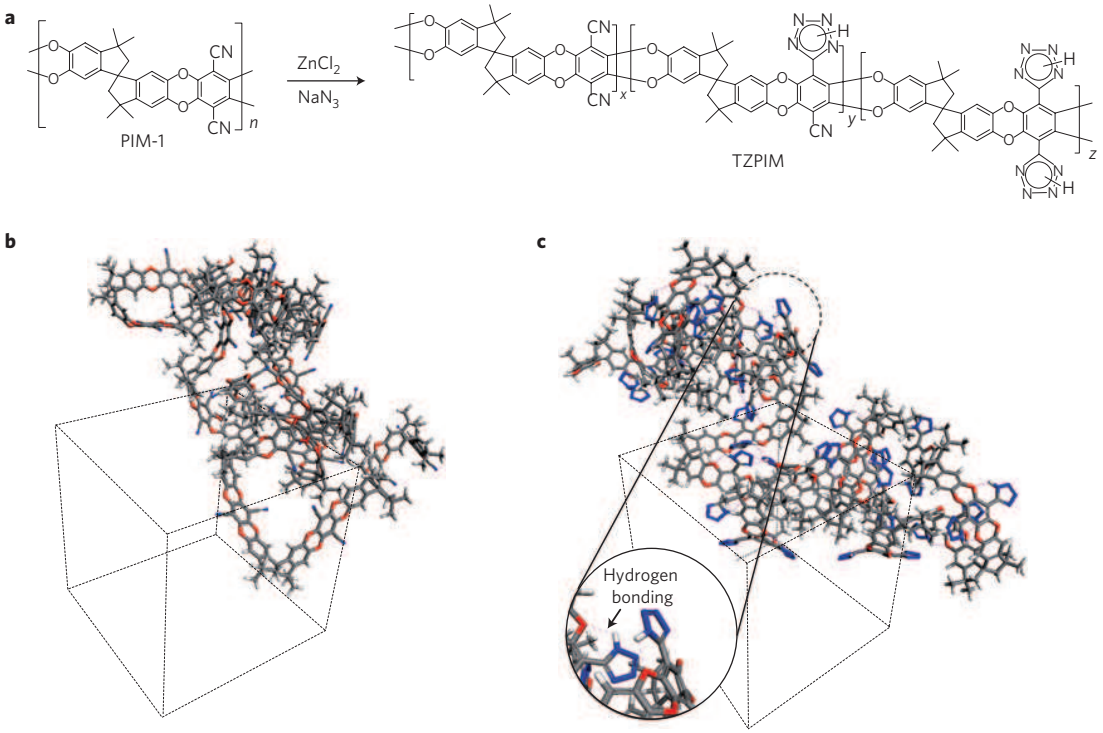

Figure 1 | Schematic illustration and computer modelling structures of PIM-1 and TZPIM. a, Conversion of PIM-1 to TZPIM via the [2+3] cycloaddition reaction between aromatic nitrile groups and sodium azide, producing a tetrazole functional group. **b**, Three-dimensional view of PIM-1 in an amorphous periodic cell (the number of repeat units is 20). **c**, Three-dimensional view of TZPIM-3 in an amorphous periodic cell (the number of repeat units is 20; 100% conversion from nitrile groups to tetrazole groups; the blue dotted line indicates possible hydrogen-bonding modes).

nitrile groups to yield low molecular weight triazole compounds[24], post-polymerization modification reactions for attaching tetrazole onto nitrile-containing aliphatic polymers (acrylonitrile-type) have in a sense been a rediscovery[24,27]. Up to now, relatively little work on the post-polymerization [2 + 3] cycloaddition modification of nitrile-containing polymers has been reported, and much of this has been on aliphatic systems such as polyacrylonitrile and its copolymers. The present work is the first reported [2 + 3] cycloaddition reaction of a polymer containing an aromatic nitrile group with an azide, resulting in tetrazole-functionalized MOPs.

Depending on the degree of cycloaddition, TZPIMs contain two, one or zero tetrazole groups and, correspondingly, zero, one or two nitrile groups per repeat unit (Fig. 1a). Nitrile to tetrazole conversion in the range of 50–100% was achieved by solution reaction of PIM-1, using different ratios of polymer to NaN_3 and $ZnCl_2$. The solubility of TZPIMs is different from PIM-1; with increasing tetrazole content, TZPIM becomes insoluble in CH_2Cl_2, THF and $CHCl_3$, whereas they dissolve in common aprotic solvents such as DMF, DMAc and NMP. Compared with the fluorescent yellow PIM-1, the TZPIM has a yellowish-brown colour. When the tetrazole content is greater than 70%, TZPIM films become slightly brittle, mainly as a result of strong chain interactions induced by tetrazole groups. A molecular modelling comparison of PIM-1 and TZPIM-3 shows hydrogen-bonding chain interactions between ether linkages and tetrazole groups (Fig. 1b,c). Details of the synthesis, characterization and molecular modeling are given in the Supplementary Information.

The TZPIM membranes demonstrate exceptional gas separation performance, surpassing the most recent upper bounds[18] of conventional and state-of-the-art polymeric membranes for the important gas pairs, such as for example the CO_2/N_2 separation shown in Fig. 2. However, a substantial hurdle exists before polymeric membranes can be used for practical CO_2 separations, such as selective CO_2 removal from flue gas, biogas refining, and natural gas sweetening. In gas mixtures, the gas selectivity is typically much lower than permselectivity from single gas permeation data because of CO_2 plasticization and/or competitive sorption effects[4]. That is, CO_2 molecules cause the polymer matrix to swell, leading to increased permeability of the slower gas beyond its pure gas permeability and resulting in reduced selectivity.

In sharp contrast, surprisingly, the mixed CO_2/N_2 selectivities in TZPIMs are higher than single gas selectivity (Fig. 3a). This can be rationalized as the preferential selective sorption of CO_2 in TZPIM being enhanced by a strong interaction with tetrazole, thereby hindering the transport of N_2 in gas mixtures. Previously, this phenomenon has only been observed in hydrocarbon (condensable gas)/light gas separation (for example, n-butane/H_2) using highly permeable PTMSP (ref. 28) and PIM-1 membranes[29]. In such high free-volume glassy polymers, condensable large gases such as butane occupy the sorption sites by a strong sorption interaction, and then exclude the sorption or passage of lighter gases. However, the present result is a rare case of a similar phenomenon occurring in CO_2/N_2 gas mixtures. For the CO_2/CH_4 mixture, the mixed CO_2/CH_4 selectivities in TZPIMs are similar to single gas selectivity (Fig. 3b), also showing there is no CO_2 plasticization effect in gas mixtures.

In comparing the CO_2/N_2 and CO_2/CH_4 mixed gas separation results, a significant observation is that the CO_2/N_2 mixed gas selectivity only slightly decreased with pressure and had much higher selectivity than single gas selectivity, whereas that of CO_2/CH_4 significantly decreased with increasing feed pressure. This is closely related to the molecular properties of the gases (that is, N_2 and CH_4) and the nature of the permeation processes. Note that diffusion coefficients of gases in polymers scale with measures of molecular size, such as kinetic diameter or critical volume (V_c), whereas gas solubilities in a polymer typically scale with measures of gas condensability, such as normal boiling point (T_b) or critical temperature. Nitrogen molecules are slightly smaller

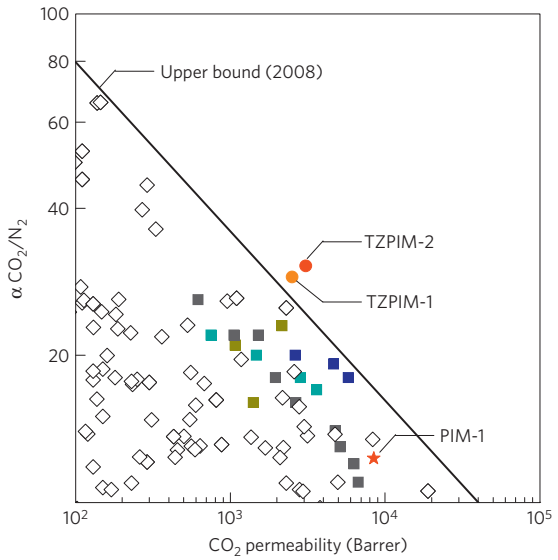

Figure 2 | Relationship between CO_2 permeability and CO_2/N_2 selectivity of TZPIMs and PIM-1. Measurements are for single gases and the upper bound is from ref. 18. TZPIM-1 (55% conversion of nitrile groups to tetrazole groups); TZPIM-2 (70.5% conversion). The squares correspond to literature data for various PIMs.

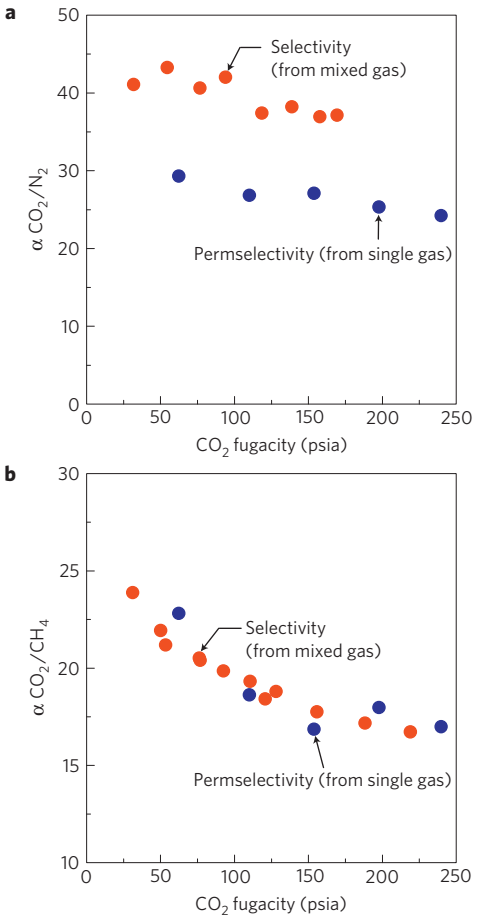

Figure 3 | Difference in single and mixed gas selectivity in TZPIM as a function of CO_2 partial pressure. a, Effect of CO_2 partial pressure on mixed-gas CO_2/N_2 selectivity in TZPIM-2 at 25 °C. Mixed gas composition (in mol% CO_2:mol% N_2) was 50:50. **b**, Effect of CO_2 partial pressure on mixed-gas CO_2/CH_4 selectivity in TZPIM-2 at 25 °C. Mixed gas compositions (in mol% CO_2:mol% CH_4) were 50:50 and 80:20. CO_2 partial pressure in the mixture was differently obtained from both such compositions.

($V_c = 93\ cm^3\ mol^{-1}$) than CH_4 ($99.3\ cm^3\ mol^{-1}$), and thus diffusion favours N_2, but CH_4 ($T_b = 112$ K) is more condensable than N_2 (77 K), and so solubility favours CH_4. In TZPIM, CH_4 permeates faster than N_2, indicating that the solubility contribution to permeability is greater than the diffusivity contribution. As such, the solubility of N_2 gas in a CO_2/N_2 mixed gas environment is considerably reduced in the presence of highly sorbing CO_2 molecules. This loss of sorption sites for N_2 molecules results in mixed gas selectivity being significantly higher than that for pure gas permselectivity. On the other hand, CH_4 molecules have greater condensability than N_2 and, therefore, still compete with CO_2 molecules in the sorption process. Without significant polymer swelling by CO_2, such behaviour in CO_2/CH_4 mixtures is also observed in CO_2 plasticization-tolerant polymers[4]. However, this is the first report of an amorphous MOP having both microporous characteristics and a high affinity for CO_2 molecules that can preferentially block N_2 molecules, thereby achieving high CO_2/N_2 mixed gas selectivity. This significant finding counters the intuitive concept that mixed gas selectivity in polymeric membranes, particularly for mixed gases containing CO_2, should be lower than pure gas selectivities because of CO_2 plasticization or competitive sorption effects.

The enhanced CO_2-philic separation properties in TZPIMs are due to interactions between CO_2 and the tetrazole. N_2 sorption isotherms at 77 K by Brunauer–Emmett–Teller (BET) in TZPIM-3 (100% conversion of nitrile to tetrazole) are comparable to common glassy polymers having low free-volume elements, and distinctly different from those in PIM-1 showing highly microporous characteristics (Fig. 4a). That is, the BET surface area in TZPIM-3 is about $30\ m^2\ g^{-1}$, which is a typical value for common glassy polymers such as polyimides[4] ($15–30\ m^2\ g^{-1}$), but markedly smaller than PIM-1 ($700\ m^2\ g^{-1}$). However, the amount of CO_2 sorption at 273 K in TZPIM-3 (Fig. 4b) is higher than that in PIM-1 in the low-pressure range, indicating that the TZPIMs have better CO_2 affinity than PIM-1, owing mainly to tetrazole groups enhancing both sorption capability and solubility-selectivity towards other gases. CO_2 sorption in the high-pressure range is given in the Supplementary Information. Thus, by improving the chemical affinity as well as by altering the microporous nature of the free-volume elements, TZPIMs can sorb CO_2 molecules more favourably than N_2 molecules. In addition, the more rigid frameworks reinforced by strong hydrogen-bonded interchain interactions may help prevent polymer swelling induced by CO_2 molecules.

Economical CO_2 capture processes offer new options for reducing greenhouse-gas emissions, in addition to the current strategies of improving energy efficiency and increasing the use of renewable energy resources. At present, the existing coal-fired power plants around the world emit about two billion tons of CO_2 in total per year. Conventional amine absorption technologies are energy intensive and costly, which would result in large incremental costs in producing electricity. Membranes offer a potentially lower cost, more energy-efficient CO_2 capture option, if highly CO_2 permeable, selective membranes exist with the feasibility to be manufactured. According to a recent estimate[30], at CO_2/N_2 selectivities above 40, a 4,000 GPU membrane ($1\ GPU = 10^{-6}\ cm^3(STP)\ (cm^2\ s\ cmHg)^{-1}$) could offer a capture cost below \$15/ton CO_2, which is lower than the US Department of Energy's (DOE) target goal of \$20/ton CO_2 (ref. 31). Based on the CO_2 permeability of a dense, thick TZPIM film (2,000 Barrers, $1\ Barrer = 10^{-10}\ cm^3(STP)\ cm\ (cm^2\ s\ cmHg)^{-1}$), if TZPIM thin-films below 0.5 μm can be successfully fabricated in the form of thin film composite membranes, and the separation performance can be verified in real flue gas compositions that include water, TZPIM

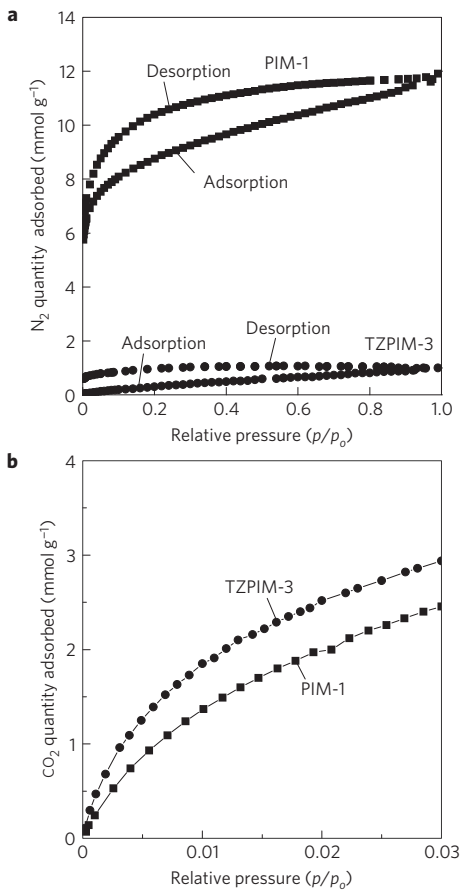

Figure 4 | Gas adsorption isotherms for PIM-1 and TZPIM-3. a, Nitrogen adsorption/desorption isotherms at −195 °C for PIM-1 and TZPIM-3 (100% conversion of nitrile groups to tetrazole groups). p/p_o is the ratio of gas pressure (p) to saturation pressure (p_o), with $p_o = 746$ torr. **b**, CO_2 adsorption isotherms at 0 °C for PIM-1 and TZPIM-3 at a low ratio of gas pressure to saturation pressure.

membranes will provide a viable energy-saving alternative for CO_2 capture from flue or fuel gas that is within current DOE cost targets.

Received 16 December 2010; accepted 17 February 2011; published online 3 April 2011

References

1. Yaghi, O. M. *et al.* Reticular synthesis and the design of new materials. *Nature* **423,** 705–714 (2003).
2. Cooper, A. I. Conjugated microporous polymers. *Adv. Mater.* **21,** 1291–1295 (2009).
3. McKeown, N. B. *et al.* Towards polymer-based hydrogen storage materials: Engineering ultramicroporous cavities within polymers of intrinsic microporosity. *Angew. Chem. Int. Ed.* **45,** 1804–1807 (2006).
4. Park, H. B. *et al.* Polymers with cavities tuned for fast selective transport of small molecules and ions. *Science* **318,** 254–258 (2007).
5. Long, T. M. & Swager, T. M. Molecular design of free volume as a route to low-k dielectric materials. *J. Am. Chem. Soc.* **125,** 14113–14119 (2005).
6. Davis, M. E. Ordered porous materials for emerging applications. *Nature* **417,** 817–821 (2002).
7. Schüth, F. & Schmidt, W. Microporous and mesoporous materials. *Adv. Mater.* **14,** 629–638 (2002).
8. Kitagawa, S., Kitaura, R. & Noro, S-I. Functional porous coordination polymers. *Angew. Chem. Int. Ed.* **43,** 2334–2375 (2004).
9. Nagai, K., Masuda, T., Nakagawa, T., Freeman, B. D. & Pinnau, I. Poly[1-(trimethylsilyl)-1-propyne] and related polymers: Synthesis, properties and functions. *Prog. Polym. Sci.* **26,** 721–798 (2001).
10. Park, H. B., Han, S. H., Jung, C. H., Lee, Y. M. & Hill, A. J. Thermally rearranged (TR) polymer membranes for CO_2 separation. *J. Membr. Sci.* **359,** 11–24 (2010).
11. Budd, P. M., McKeown, N. B. & Fritsch, D. Polymers of intrinsic microporosity (PIMs): High free volume polymers for membrane applications. *Macromol. Sym.* **245,** 403–405 (2006).
12. Côté, A. P. *et al.* Porous, crystalline, covalent organic frameworks. *Science* **310,** 1166–1170 (2005).
13. El-Kaderi, H. M. *et al.* Designed synthesis of 3D covalent organic frameworks. *Science* **316,** 268–272 (2007).
14. Budd, P. M. *et al.* Gas separation membranes from polymers of intrinsic microporosity. *J. Membr. Sci.* **251,** 263–269 (2005).
15. Du, N. Y., Robertson, G. P. & Guiver, M. D. Polymers of intrinsic microporosity derived from novel disulfone-based monomers. *Macromolecules* **42,** 6023–6030 (2009).
16. Du, N. Y., Robertson, G. P., Song, J. S. & Guiver, M. D. High-performance carboxylated polymers of intrinsic microporosity (PIMs) with tunable gas transport properties. *Macromolecules* **42,** 6038–6043 (2009).
17. Du, N. Y. *et al.* Polymers of intrinsic microporosity containing trifluoromethyl and phenylsulfone groups as materials for membrane gas separation. *Macromolecules* **41,** 9656–9662 (2008).
18. Robeson, L. M. The upper bound revisited. *J. Membr. Sci.* **320,** 390–400 (2008).
19. Lin, H. & Freeman, B. D. Materials selection guideline for membranes that remove CO_2 from gas mixtures. *J. Mol. Struct.* **739,** 57–74 (2005).
20. Lin, H. & Freeman, B. D. Gas solubility, diffusivity and permeability in poly(ethylene oxide). *J. Membr. Sci.* **239,** 105–117 (2004).
21. Vogiatzis, K., Mavrandonakis, A., Klopper, W. & Froudakis, G. E. *Ab initio* study of the interactions between CO_2 and N-containing organic heterocycles. *ChemPhysChem* **10,** 374–383 (2009).
22. Gothelf, K. V. & Jørgensen, K. A. Asymmetric 1,3-dipolar cycloaddition reactions. *Chem. Rev.* **98,** 863–910 (1998).
23. Huisgen, R., Szeimies, G. & Möbius, L. 1,3-Dipolar cycloadditions. XXXII. Kinetics of the addition of organic azides to carbon-carbon multiple bonds. *Chem. Ber.* **100,** 2494–2507 (1967).
24. Binder, W. H. & Sachsenhofer, R. Click chemistry in polymer and materials science. *Macromol. Rapid Commun.* **28,** 15–54 (2007).
25. Guiver, M. D., Robertson, G. P., Yoshikawa, M. & Tam, C. M. Functionalized polysulfones: Methods for chemical modification and membrane applications. *ACS Symp. Ser.* **744,** 137–161 (2000) Chapter 10.
26. Guiver, M. D. & Robertson, G. P. US Patent 5,475,065 (1995).
27. Tsarevsky, N. V., Bernaerts, K. V., Dufour, B., Du Prez, F. E. & Matyjaszewski, K. Well-defined (co)polymers with 5-vinyltetrazole units via combination of atom transfer radical (co)polymerization of acrylonitrile and click chemistry-type postpolymerization modification. *Macromolecules* **37,** 9308–9313 (2004).
28. Pinnau, I., Casillas, C. G., Morisato, A. & Freeman, B. D. Hydrocarbon/hydrogen mixed gas permeation in poly(1-trimethylsilyl-1-propyne) (PTMSP), poly(1-phenyl-1-propyne) (PPP), and PTMSP/PPP blends. *J. Polym. Sci. Polym. Phys.* **34,** 2613–2621 (1996).
29. Thomas, S., Pinnau, I., Du, N. & Guiver, M. D. Hydrocarbon/hydrogen mixed-gas permeation properties of PIM-1, an amorphous microprous spirobisindane polymer. *J. Membr. Sci.* **338,** 1–4 (2009).
30. Merkel, T., Lin, H., Wei, X. & Baker, R. Power plant post-combustion carbon dioxide capture: An opportunity for membranes. *J. Membr. Sci.* **359,** 126–139 (2010).
31. Figueroa, J. D., Fout, T., Plasynski, S., McIlvried, H. & Srivastava, R. D. Advances in CO_2 capture technology—the US Department of Energy's Carbon Sequestration Program. *Int. J. Greenhouse Gas Control* **2,** 9–20 (2008).

Acknowledgements

NRCC No. 52847. The authors acknowledge partial support from the Climate Change Technology and Innovation Initiative, Greenhouse Gas project (CCTII, GHG), Natural Resources Canada (NRCan) and from Vaperma. H.B.P. and M.D.G. acknowledge support by the WCU (World Class University) programme through the National Research Foundation of Korea, funded by the Ministry of Education, Science and Technology (No. R31-2008-000-10092-0). The authors are very grateful to F. Toll of the National Research Council for the BET absorption measurements.

Author contributions

N.D. experimental design, synthesis and gas permeation experiments, data analysis, manuscript writing; H.B.P. computer modeling, gas permeation and gas adsorption experiments, data analysis, manuscript writing; G.P.R. NMR and TGA-MS experiments, data analysis; M.M.D-C. gas permeation experiments, data analysis; T.V. industrial application input; L.S. assisted in the synthetic experiments; M.D.G. project idea, direction and supervision, experimental design, data analysis, manuscript writing.

Additional information

The authors declare no competing financial interests. Supplementary information accompanies this paper on www.nature.com/naturematerials. Reprints and permissions information is available online at http://npg.nature.com/reprintsandpermissions. Correspondence and requests for materials should be addressed to M.D.G.

nature materials

SUPPLEMENTARY INFORMATION

DOI: 10.1038/NMAT2989

Polymer nanosieve membranes for CO_2-capture applications

Naiying Du[1], Ho Bum Park[2], Gilles P. Robertson[1], Mauro M. Dal-Cin[1], Tymen Visser[3], Ludmila Scoles[1], Michael D. Guiver[1,2*]

[1]Institute for Chemical Process and Environmental Technology, National Research Council of Canada, Ottawa, Ontario K1A 0R6, Canada
[2]WCU Department of Energy Engineering, Hanyang University, Seoul 133-791, Republic of Korea
[3]Vaperma, 2111, 4e rue, St-Romuald, Québec, G6W 5M6, Canada

*Corresponding Author. (michael.guiver@nrc-cnrc.gc.ca)

Materials and Methods

1. Materials

Dimethylacetamide (DMAc), N-methylpyrrolidone (NMP), toluene, methanol (MeOH), potassium carbonate (K_2CO_3), sodium azide (NaN_3), zinc chloride ($ZnCl_2$), and chloroform ($CHCl_3$) were purchased from Sigma-Aldrich and used as received. 5,5',6,6'-Tetrahydroxy-3,3,3',3'-tetramethylspirobisindane (TTSBI, Sigma-Aldrich) was purified by crystallization from methanol. Tetrafluoroterephthalonitrile (TFTPN, Matrix scientific) was purified by vacuum sublimation at 150°C under an inert atmosphere.

2. Synthesis of TZPIM

PIM-1 was dissolved in NMP (1-3 g in 20 mL of solvent). NaN_3 and anhydrous $ZnCl_2$ with different mol equiv. versus the nitrile groups were added, and the mixture was stirred at 120 °C for different reaction times according to the conversion required (See Table 1). After cooling to 60 °C, 15 mL of diluted HCl (1:50 by volume in water) was added, and

DOI: 10.1038/NMAT2989

the reaction mixture was maintained at this temperature for 3 - 5 h. The PIMs thus obtained were then precipitated into excess 1 M HCl, filtered, washed on the filter with dilute HCl and water, and dried in a vacuum oven at 120 °C. Elem. Anal. Calculated for $C_{29}H_{22}N_8O_4$ (the fully-substituted tetrazole PIMTZ-3 from the 8 d reaction): N, 20.50%; Found: N, 19.14%.

Table 1. Properties of PIM-1 and TZPIM films modified under different conditions

Sample No.	-CN / NaN_3 / $ZnCl_2$	Reaction time	Conversion *	M_n *
PIM-1	/	/	0	58,000
TZPIM-1.	1 : 4 : 2	2 d	55%	52,000
TZPIM-2.	1 : 4 : 4	2 d	70.5%	45,000
TZPIM-3.	1 : 4 : 4	8 d	100%	34,000

* Conversion is the molar ratio of the tetrazole groups in the TZPIM to the total nitrile groups of PIM-1, which is based on the ^{1}H NMR calculation of the integration ratio of the methyl signal of a methylated derivative of TZPIM to the methyl signals of the ladder polymer backbone. M_n values were obtained from the GPC curves of the corresponding methylated TZPIM derivatives. The details of the methylation procedure will be published elsewhere.

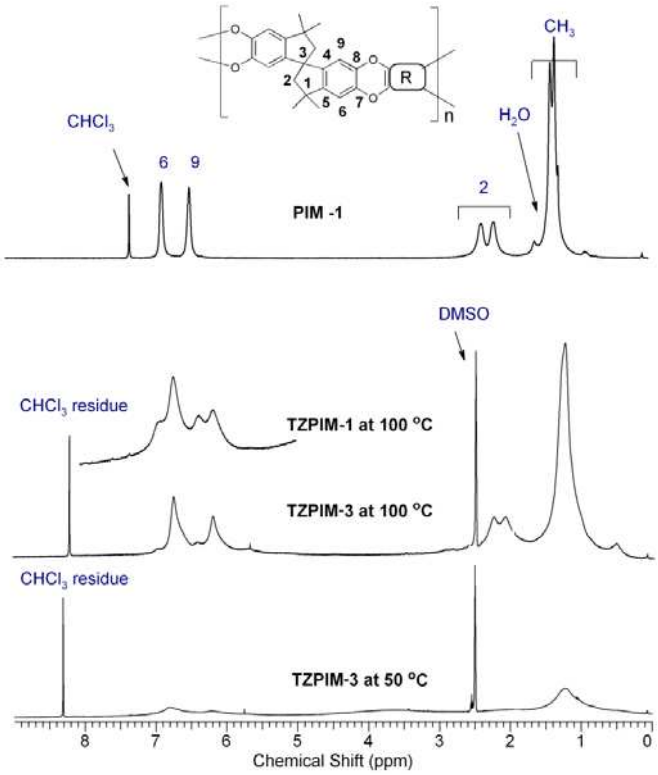

Fig. 1. Comparative ^{1}H NMR spectra of PIM-1, TZPIM-1 and TZPIM-3

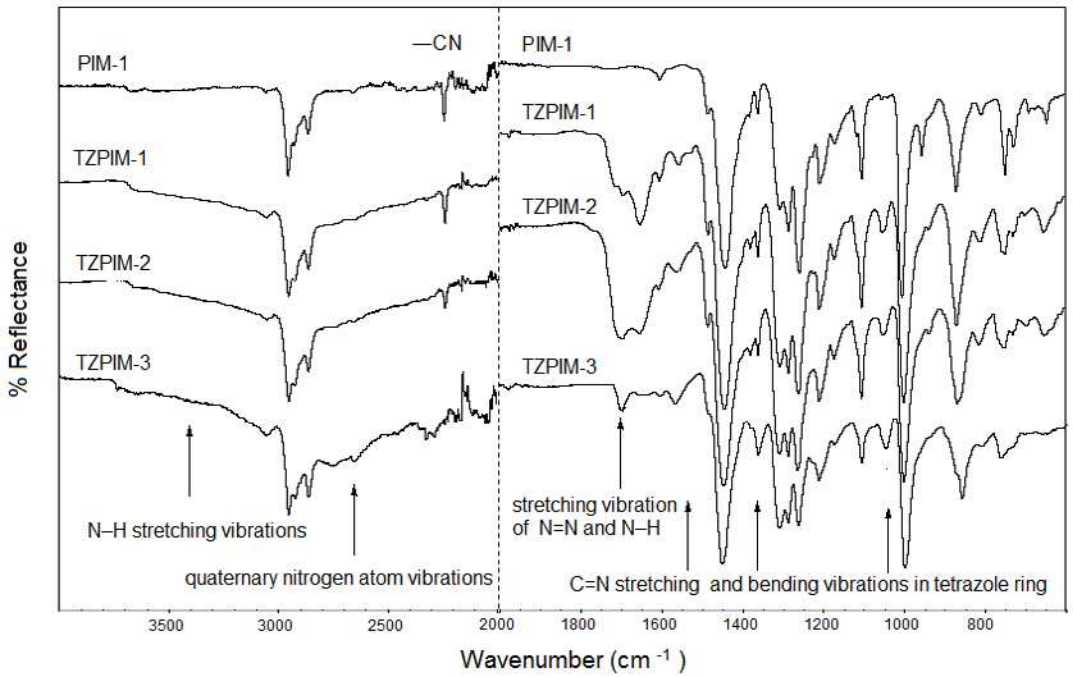

Fig. 2. Comparative FTIR spectra of PIM-1 and TZPIM-1 to -3

3. Methods

The structures of the polymeric materials were fully characterized using nuclear magnetic resonance (NMR) spectroscopy at different temperatures. NMR analyses were recorded on a Varian Unity Inova spectrometer at a resonance frequency of 399.961 MHz for ^{1}H and 376.276 MHz for ^{19}F. ^{1}H and ^{19}F NMR spectra were obtained from samples dissolved in $CDCl_3$ or DMSO-d_6 using a 5 mm pulsed field gradient indirect detection probe. The solvent signals ($CDCl_3$ ^{1}H 7.25 ppm; DMSO-d_6 ^{1}H 2.50 ppm) were used as the internal references. ^{19}F NMR (external reference $CFCl_3$ 0 ppm) was used to confirm the integrity of the ladder structure. Molecular weight and molecular weight distributions were measured by GPC using Ultrastyragel columns and THF as the eluent at a flow rate of 1 mL/min. The values obtained were determined by comparison with a series of polystyrene standards. FTIR

DOI: 10.1038/NMAT2989

spectra of films were recorded on Thermo Scientific FTIR spectrum (model Nicolet 6700) at 4 cm^{-1} resolution over the 400-4000 cm^{-1} range. Each sample was scanned 64 times. Elemental analysis was carried out by Galbraith Laboratories. Inc. Gas sorption measurements were performed using an ASAP 2020 (Accelerated Surface Area and Porosimetry System) from Micromeritics Instrument Corporation. Data analysis was performed using the ASAP 2020 version 3 software Rev H. High-purity gases were used for analysis. The polymer powders were degassed under high vacuum at 80°C for 24 h prior to measurement. Polymer thermal degradation curves were obtained from thermogravimetric analysis (TGA) (TA Instruments, model Q-5000IR). Polymer samples for TGA were initially heated to 150 °C under nitrogen gas and maintained at that temperature for 1 h for moisture removal and then heated to 600 °C at 10 °C/min for degradation temperature measurement. The TGA furnace was equipped with an interface for a mass spectrometer, MS model Thermostar from Pfeiffer Vacuum, which was used to detect gas driven off from thermally degraded samples in the TGA instrument.

NMR spectra of PIM-1 in $CDCl_3$, TZPIM-1 and TZPIM-3 in DMSO-d_6 are shown in Fig. 1 with signal assignments, which were derived unambiguously from 2D-NMR. The intensities and the shapes of the TZPIM3 polymer ^1H NMR signals were monitored at different NMR probe temperatures, to observe hydrogen bonding temperature dependence. The observed signal intensity ratio (at 100 ^oC) for the TZPIM-33 aromatic (6.73, 6.19 ppm, H-6, 9) and aliphatic (0.25-2.4 ppm, H-2 and CH_3) regions was exactly 4H : 16H, as expected from the molecular structure. Signals in the region of 0.5-7.0 ppm increased with increasing temperature. In addition, four signals of TZPIM-1 at 6.92, 6.73, 6.35 and 6.19 ppm show the shielding effects of –CN and tetrazole groups, which provides evidence for the conversion of

–CN to tetrazole groups after the [2 + 3] cycloaddition reaction.

The FTIR spectrum (Fig. 2) of PIM-1 shows the characteristic nitrile absorption band at 2238 cm^{-1}, and the absence of bands in the range of 3000 to 3600 cm^{-1}, indicating no N–H group is present. After cycloaddition reaction, broad absorption bands are observed in samples TZPIM 1-3 in the range of 3000 to 3600 cm^{-1}, corresponding to N–H stretching vibrations with hydrogen bonding (N–H•••N), and in the range of 2300 to 2800 cm^{-1}, attributed to vibrations of quaternary nitrogen atom. An intense absorption at 1580 cm^{-1} arises due to stretching vibration of the N=N and N–H groups, which implies that some of the nitrile groups were converted into tetrazole groups. Bands near 1510, 1400, and 1100 cm^{-1} are characteristic of C=N stretching and bending vibrations of the tetrazole ring, respectively.

None of the PIMs had a discernable T_g in the measured range of 50 °C to 350 °C, due to the absence of rotational freedom of the main chain. The TZPIMs decomposed at lower temperatures compared to PIM-1; the initial degradation step of the tetrazole ring was ~170 °C, and the second main-chain degradation occurred at ~488 °C. MS analysis of the decomposition products of TZPIM3, using 30 mL/min of He as the purge gas and 5 ^{o}C/min ramping rate, showed m/e 14, 28 and 29, indicative of nitrogen gas detected by MS. At a higher heating rate of 10 °C/min, explosive decomposition of the polymer was observed between 170 ^{o}C and 300 ^{o}C. The initial N_2 decomposition product is formed by extrusion from tetrazole groups. Furthermore, the ~14.6 % initial step weight loss for TZPIM3 is close to the ~15% calculated weight loss that would occur from complete tetrazole decomposition, which provides further evidence for the complete conversion of nitrile to tetrazole structures.

DOI: 10.1038/NMAT2989

4. Membranes

Dense polymer films for gas permeability measurements were prepared from 1-2 wt% PIM solutions in chloroform or DMAc. Solutions of PIM-1 and tetrazole-modified PIM were filtered through 0.45 μm polypropylene filters and then poured onto glass (for PIM-1) or Teflon Petri dishes (for TZPIM) in a glove box at room temperature (for $CHCl_3$) or 80^{o}C (for DMAc) and allowed to evaporate slowly for 1 day. The membranes were boiled in water first (with HCl, pH = 4 - 5). After several washes in water, the membranes were soaked in methanol and dried in a vacuum oven at 120°C for 24 h. The resulting flexible (except TZPIM3) membranes with thickness in the range of 70-90 μm were bright yellow (for PIM-1) or brownish yellow (TZPIM).

The polymer membranes were tested for pure and mixed gas permeabilities using cross-flow cells with a permeation area of 9.62 cm^2. Gases were obtained from BOC, air was dry and CO_2 free grade, O_2 and N_2 were UHP grade or equivalent, CO_2 was bone dry grade. Feed mixtures of CO_2/N_2 were prepared at 20, 30 and 40% using mass flow controllers (1179 MKS), via a flow controller 247C with CO_2 set to a ratio of the N_2 flow. Feed and permeate concentrations for CO_2 were measured using a Quantek 906 CO_2 analyzer with a 0-100% range. Oxygen concentrations for air permeation experiments were measured using an Advanced Micro Instruments O_2 meter, Model 65, calibrated to 20.9% oxygen for air with a range of 0-95%. Permeate flows were measured using an Agilent ADM 2000 flowmeter with a range of 0.5 to 1000 mL/min or a bubble flow meter with a range of 0.1 to 10 mL. Permeabilities are corrected to standard temperature and pressure from a typical room temperature of 22 °C. Membranes were initially evaluated using air and allowed to stabilize overnight. Pure gas permeabilities were typically measured in the sequence N_2, O_2, CO_2, with

a 0.34 MPa pressure difference (50 psi) and with the permeate at atmospheric pressure. Mixtures were measured in increasing CO_2 feed concentrations and the pure gas sequence repeated in selected cases. Feed flows with mixed gases were maintained at 1,500 mL min^{-1} and the permeate recovery was generally maintained below 2%.

High pressure CO_2 sorption measurements of TZPIM-1 and TZPIM-2 are shown in Fig. 3.

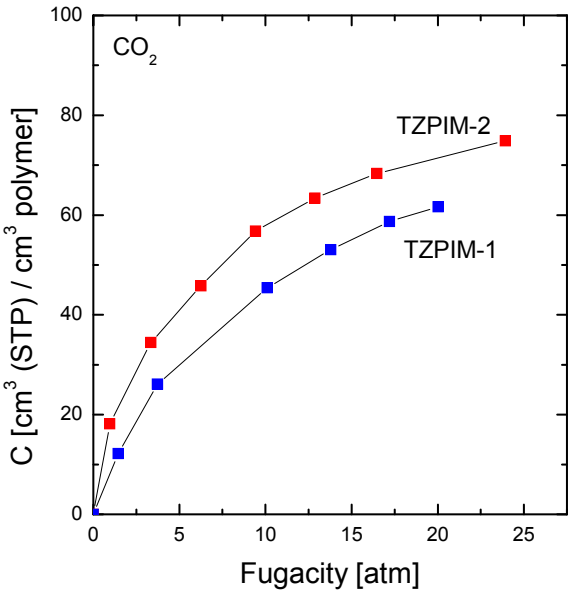

Fig. 3. High pressure CO_2 sorption of TZPIM-1 and TZPIM-2

5. Molecular Modeling

For the simulated polymer cells of PIM-1 and TZPIM-3 shown in Figures 1b and 1c, all of the molecular simulations were performed using a Hewlett Packard workstation and the Material Studio software package (Accelrys Inc, CA, USA). For simulation, the commercial force field COMPASS was used. PIM-1 and TZPIM-3 chains with 30 repeat units were built

DOI: 10.1038/NMAT2989

and amorphous models were constructed at 298K under periodic boundary conditions using Amorphous Cell module in Material Studio 4.2. Successive iterations of energy-minimization (via the smart minimizer method, which is a combination of the steepest descent, conjugated gradient and Newton methods in a cascade, where the convergence levels were set to 1000 kcal mol^{-1} $Å^{-1}$, 10 kcal mol^{-1} and 0.1 kcal mol^{-1}, respectively) and molecular dynamics (molecular dynamics (MD) simulations were performed using a time step of 1.0 fs for equilibrating the cells and obtaining the final densities. The Ewald summation method was used to calculate the non-bond interactions (electrostatic and van der Waals) with an accuracy of 0.001 kcal mol^{-1}. The Berendsen algorithm, set to a decay constant of 0.1 ps, was used to control the temperature and pressure of each cell, including compression and structural relaxation. The algorithm was performed until the density of each polymer chain converged and the system was stable, with no large density fluctuations at 1 bar. The average calculated densities, using at least ten amorphous cells, were 1.057 (for PIM-1) and 1.331 (for TZPIM-3) gcm^{-3}, respectively. These calculated values were close to the experimental densities (1.063 and 1.339 gcm^{-3}). Specific MD simulation procedures are as follows: (1) NPT (a constant particle number, pressure and temperature) MD simulation at 400 K and 1 bar for 50 ps, (2) NPT MD simulation at 298 K and 1 bar for 50 ps and (3) NVT (a constant particle number, volume and temperature) MD simulation at 298 K for 10 ps. After comparing the simulated and the experimental densities, most PIM-1 and TZPIM-3 amorphous cells had about 10% lower values, and therefore further MD simulations were performed: (4) NPT MD simulation at 298 K and 10000 bar for 50 ps, (5) NVT MD simulation at 600 K for 20ps, (6) NVT MD simulation at 298 K and for 20 ps and (6) NPT MD simulation at 298 K and 1 bar for 50 ps. Step (4)-(7) were repeated until the simulated density changing rates had converged

to within 3%. Finally, NVT MD simulation was performed at 298 K for 10 ps for production of the PIM-1 and TZPIM-3 models. In TZPIM-3, the hydrogen bonds were automatically detected using a hydrogen bond search program in a 3D atomistic periodic box. The calculated bond energy ranges from 1 kcal/mol to 5 kcal/mol.